Trichlorfon induces apoptosis in SH-SY5Y neuroblastoma cells via the endoplasmic reticulum?

Cheng-Yun Liu [a,b], Ping-An Chang [a], Yi-Jun Wu [a,*]

[a] Laboratory of Molecular Toxicology, State Key Laboratory of Integrated Management of Pest Insects and Rodents, Institute of Zoology, Chinese Academy of Sciences, Datunlu Road, Beijing 100101, PR China
[b] Graduate School of the Chinese Academy of Sciences, Beijing 100039, PR China

ARTICLE INFO

ABSTRACT

This study investigated the role of the endoplasmic reticulum pathway in apoptosis induced by trichlorfon in SH-SY5Y human neuroblastoma cells. Flow cytometric analysis demonstrated that trichlorfon and its degradation product dichlorvos-induced apoptosis in a dose-dependent manner and Hoechst 33342 staining experiments revealed trichlorfon/dichlorvos-induced nucleus condensation. Western blot analysis indicated decreased expression of caspase-12 and increased activated caspase-12 in trichlorfon-treated cells compared to a control, suggesting that trichlorfon may induce apoptosis in SH-SY5Y partly via the endoplasmic reticulum. Intracellular Ca^{2+} level ($[Ca^{2+}]_i$) in SH-SY5Y cells increased after treatment with trichlorfon but was significantly reduced by pre-treatment with a combination of a calcium channel blocker, an inositol trisphosphate receptor inhibitor, and a ryanodine receptor inhibitor. Percent apoptosis and activated caspase-3 and caspase-12 decreased in pre-treated cells compared to those treated with trichlorfon alone. Trichlorfon-induced apoptosis was also inhibited by the protein kinase C activator, phorbol 12-myristate 13-acetate (PMA). These results suggest that endoplasmic reticulum stress, which is related to calcium, may be involved in the cytotoxicity of trichlorfon.

© 2009 Elsevier Ireland Ltd. All rights reserved.

1. Introduction

Organophosphorus (OP) compounds are used in large amounts over extensive area, causing environmental pollution and risk to human health. Trichlorfon [O,O-dimethyl-(2,2,2-trichloro-1-hydroxyethyl)], a kind of OPs, has been used as an insecticide on a large scale in crop protection and in the field of hygiene since 1952. In veterinary medicine it has been used against ecto- and endoparasites and in aquaculture against salmon lice [1]. In human medicine trichlorfon (metrifonate) was used in the treatment against schistosomiasis, and it was in clinical trials for symptomatic treatment of Alzheimer's disease in the 20th century [2,3]. When incorporated into an organism, trichlorfon is rapidly dechlorinated to dichlorvos, which is a more potent inhibitor of cholinesterases [4].

The clinical signs and symptoms associated with acute trichlorfon poisoning are generally attributable to acetylcholine accumulation following the inhibition of acetylcholinesterase (AChE). In addition to acute cholinergic effects, trichlorfon is capable of causing a progressive delayed neurological deficit called organophosphate-induced delayed neurotoxicity (OPIDN), as well as chronic symptoms that persists for years after exposure and is distinct from both cholinergic and OPIDN effects in both humans and animals [5]. There has been a report of cluster of human birth defects (mainly chromosomal trisomy) presumably caused by eating fish shortly after its exposure to a trichlorfon-containing delousing compound [6]. Other studies have shown that trichlorfon can be regarded as a germ cell aneugen [7,8], which is related to the chronic toxicity of trichlorfon. In addition, some studies reported that trichlorfon caused toxicity via production of free radicals and impairing antioxidant system, besides its typical action as an inhibitor of AChE [9,10]. Mehl et al. [11] found that both light and electron microscopic changes in cerebellar cortex after trichlorfon treatment were characteristic of apoptosis and an increased level of apoptosis after trichlorfon treatment. However, the mechanism involved in this process remains unclear. In this study, we selected the SH-SY5Y human neuroblastoma cell line as a model system for trichlorfon toxicity testing and studied the mechanism involved in the trichlorfon-induced cell death.

2. Materials and methods

2.1. Chemicals

Fura-2-AM, verapamil, 2-aminoethoxydiphenyl borate (2-APB), ruthenium red, and Hoechst 33342 were obtained from Sigma Chemical Company (St. Louis, MO, USA). Phorbol 12-myristate

* Corresponding author. Tel.: +86 10 64807251; fax: +86 10 64807099.
E-mail address: wuyj@ioz.ac.cn (Y.-J. Wu).

13-acetate (PMA) was obtained from Fluka (Buchs, Switzerland). Trichlorfon (99.5%) and dichlorvos (99%) were purchased from Shanghai Biochemical Reagent Co. Ltd. (Shanghai, China). Dulbecco's modified Eagle's medium (DMEM) was obtained from Gibco (Grand Island, NY, USA). Fetal bovine serum (FBS) was purchased from the Chinese Academy of Medical Sciences (Beijing, China) and trypsin from Amresco (Solon, OH, USA). Antibodies of anti-caspase-3, Bcl-2, p53, and actin were obtained from Santa Cruz Biotechnology (Santa Cruz, CA, USA). Anti-caspase-12 antibody was obtained from Stressgen (Glanford, Victoria, Canada).

2.2. Cell culture and treatment

SH-SY5Y human neuroblastoma cells were obtained from the Cell Center of the Chinese Academy of Medical Sciences (Beijing, China). Cells were cultured as described by Ehrich and Veronesi [12]. SH-SY5Y cells were grown in DMEM supplemented with 10% (v/v) FBS, 100 units/ml penicillin, and 100 µg/ml streptomycin. Prior to confluence, cells were harvested using 0.25% trypsin and seeded onto plastic culture dishes (Corning Glass Works, Corning, NY, USA), at 4×10^5 cells/ml. The cells were then allowed to grow at 37 °C in humidified 5% CO_2/95% air for 24 h prior to treatment.

2.3. Cell viability assay

Cell viability was estimated by a colorimetric method, which is based on the ability of cellular dehydrogenases of viable cells to reduce MTT [3-(4, 5-dimethylthiazol-2-yl)-2, 5-diphenyl tetrazolium bromide] from a yellow water soluble dye to a dark blue insoluble formazan product. SH-SY5Y cells were seeded in 96-well plates at 1×10^4 cells/well (100 µl) and allowed to attach for 24 h. The cells were then treated with trichlorfon or dichlorvos and returned to the incubator for 48 h. MTT was added to the medium at the concentration of 0.5 mg/ml and incubated for 4 h. Then, 100 µl DMSO and 50 µl glycine containing 100 mM NaCl (pH10.5) were added to all wells and the plate was shaken for 10 min to dissolve the crystal. The plates were read with a Bio-Rad Benchmark microplate reader (Hercules, CA, USA) at wavelength of 570 nm. Controls included untreated cells and pure medium, with all MTT assays performed in triplicate.

2.4. Fluorescence microscopy of nuclear morphology

Apoptosis is easily determined by the visualization of late-stage DNA's fragmentation into DNA particles [13]. This is achieved by fluorescently labeling DNA with DNA-specific dyes [14]. SH-SY5Y cells were exposed to trichlorfon (200 µM) or dichlorvos (20 µM) for 48 h, washed twice with phosphate-buffered solution (PBS) (200 mM NaCl, 2.7 mM KCl, 10 mM Na_2HPO_4, 1.8 mM KH_2PO_4, pH 7.4) and fixed with ice-cold 90% (v/v) methanol in Tris-buffered solution (TBS) (50 mM Tris–HCl and 150 mM NaCl, pH 7.4) for 15 min. Then cells were stained with the DNA-specific fluorochrome Hoechst 33342 (10 µg/ml) for 15 min. Stained cells were evaluated visually for apoptotic nuclear fragmentation.

2.5. Analysis of apoptosis by flow cytometry

Apoptosis in SH-SY5Y cells subjected to various treatments was determined using an annexin V-FITC (fluorescein isothiocyanate) staining kit from Baosai Biosciences (Beijing, China). Propidium iodide (PI) was used to differentiate apoptotic cells with membrane integrity (annexin+/PI−) from necrotic cells that had lost membrane integrity (annexin+/PI+). The assay was performed following the manufacturer's recommended procedure. After staining, the percentage of apoptotic cells under various treatments was analyzed

with a Becton Dickinson FACScan flow cytometer (San Jose, CA, USA).

2.6. AChE assay

The AChE assay was performed as described by Gorun et al. [15]. In brief, cells were washed twice with PBS, harvested, and suspended in 20 mM PBS after centrifugation, homogenized with 10 passages through a 25-gauge hypodermic needle, and centrifuged at $400 \times g$ for 3 min and the supernatant was collected. Then 10 µl of 40 mM acetylthiocholine iodide was added to 100 µl supernatant. This reaction mixture was incubated at 37 °C for 30 min, and the reaction was stopped with 990 µl of 0.125 mM DTNB–phosphate–ethanol reagent (12.4 mg DTNB, 120 ml 96% alcohol, 80 ml H_2O, 50 ml 0.1 M PBS, pH 7.6). The absorbance was measured at the wavelength of 412 nm.

2.7. Measurement of the intracellular Ca^{2+} level

$[Ca^{2+}]_i$ was determined using the Ca^{2+}-sensitive fluorescent indicator Fura-2/AM and monitored as described by Li and Wu [16]. The cells were washed with HEPES-buffered medium (140 mM NaCl, 5 mM KCl, 1 mM Na_2HPO_4, 1 mM $MgCl_2$, 1 mM $CaCl_2$, 1 mg/ml glucose and 20 mM HEPES, pH 7.4), then incubated with 4 µM Fura-2/AM for 40 min at 37 °C. After two washes, cells were suspended in supplemented HEPES buffer. Cells were transferred to a water-jacketed cuvette (1.6×10^6 cells/cuvette) and the Fura-2 fluorescence was then measured with a Hitachi F-4500 fluorescence spectrophotometer (Tokyo, Japan). Excitation signals were recorded at 340 nm and 380 nm and the emission signal at 510 nm at 1-s intervals. Maximum and minimum fluorescence values (F_{max} and F_{min}) were obtained by adding 10 µM Triton X-100 and 5 µM EGTA, respectively. $[Ca^{2+}]_i$ were calculated according to the equation $[Ca^{2+}]_i = K_d(F - F_{min})/(F_{max} - F)$, where K_d is the apparent dissociation constant (224 nM) of the fluorescent dye-Ca^{2+} complex.

2.8. Western blotting analysis

Cells were harvested, washed twice with PBS, and suspended in a lysis buffer as previously described [17]. The cells were lysed by four repeated cycles of freezing and thawing, and then centrifuged at 4 °C for 30 min at $12,000 \times g$. The supernatant was collected and either stored at −80 °C or used immediately. The samples were analyzed for total protein using the Bradford method [18]. Cell lysates (50 µg protein per well) were separated on 12% SDS-polyacrylamide gels and electroblotted onto a nitrocellulose membrane (Amersham, Piscataway, NJ, USA) using standard techniques as described by Masoud et al. [19]. After electrophoretic transfer, the membranes were blocked by incubation for 1 h in PBS buffer containing 5% nonfat dry milk and 0.1% Tween-20. The blots were then incubated overnight at 4 °C with one of the following polyclonal antibodies: anti-caspase-3 (1:1000), anti-caspase-12 (1:2000), anti-p53 (1:1000). The blots were then incubated with appropriate horseradish peroxidase-conjugated secondary antibodies (1:2000). The antigen–antibody complex on the blots was detected using a SuperSignal chemiluminescence kit (Pierce Biotechnology, Rockford, IL, USA) as described in the manufacturer's protocol, and visualized using a ChemiDoc XRS system (Bio-Rad, Munich, Germany). To confirm equal loading of proteins, the blots were also immunoprobed with a rabbit polyclonal antibody against the cytoskeletal protein actin (1:2000 dilution).

2.9. Statistical analysis

Data are expressed as mean ± standard deviation (S.D.) unless otherwise stated. Statistically significant differences between the

Table 1
Effects of trichlorfon and dichlorvos on viability of SH-SY5Y cells.

Trichlorfon/dichlorvos concentrations (μM)	Cell viability	
	Trichlorfon	Dichlorvos
1	–	0.98 ± 0.09
2.5	–	0.90 ± 0.11
5	–	0.84 ± 0.08
10	1.01 ± 0.11	0.75 ± 0.07
20	0.93 ± 0.07	$0.64 \pm 0.07^{*}$
50	0.82 ± 0.08	$0.31 \pm 0.06^{*}$
100	0.77 ± 0.08	–
200	$0.67 \pm 0.05^{*}$	–
500	$0.12 \pm 0.02^{*}$	–

* $p < 0.05$ compared to control.

treatments and the control were determined by one-way analysis of variance (ANOVA). A difference between means was considered significant at *$p < 0.05$.

3. Results

3.1. MTT assay

Cellular viability was assessed by MTT assay after 48 h of incubation with 10–500 μM of trichlorfon or 0.1% DMSO (v/v) as a control. The MTT assay indicated that addition of 10–100 μM of trichlorfon had no significant effect on cell viability after 48 h of incubation (Table 1). However, the addition of 200 and 500 μM of trichlorfon markedly decreased the viability of cells compared to the control, suggesting that trichlorfon inhibits cell growth in a dose-dependent manner. Since trichlorfon can be easily hydrolyzed non-enzymatically into dichlorvos, we also determined effects of dichlorvos on the cell viability in SH-SY5Y cells. MTT results indicated that 20 and 50 μM dichlorvos markerdly decreased the viability of cells compared with the control (Table 1), which indicates that trichlorfon is less toxic than its hydrolytic degradation product dichlorvos, to SH-SY5Y cells.

3.2. Trichlorfon-induced apoptosis in SH-SY5Y cells

In order to confirm that the apoptosis observed in SH-SY5Y cells was induced by trichlorfon, we counted the number of annexin V-positive/PI-negative and annexin V-positive/PI-positive, staining cells after incubation with different concentrations of trichlorfon for 48 h. This confirmed that trichlorfon-induced apoptosis in a dose-dependent manner (Fig. 1A–E). Percent apoptosis in cells treated with 50 and 100 μM trichlorfon was not significantly different to that of the control group. Higher concentrations of trichlorfon up to 200 μM caused a significant increase in the percentage of
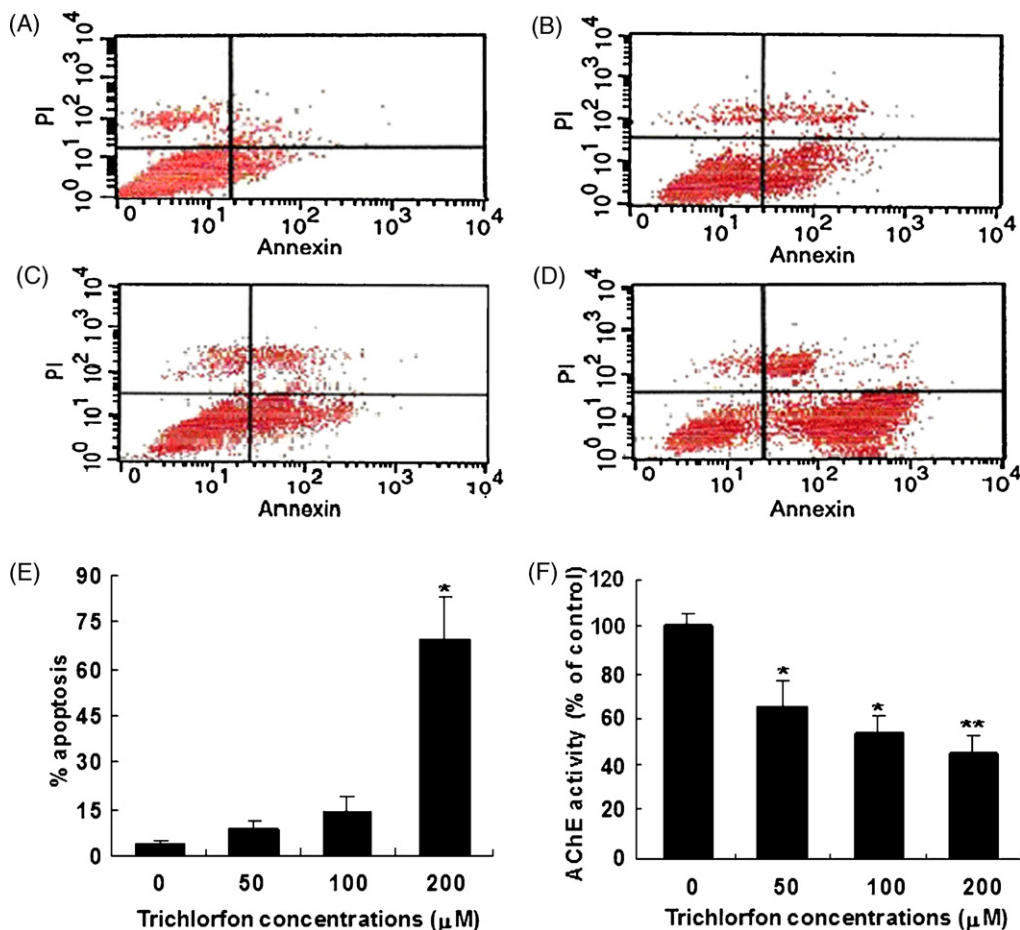

Fig. 1. Induction of apoptosis and inhibition of AChE activity by trichlorfon in a dose-dependent manner. After cells were treated with a range of concentrations (0–200 μM) of trichlorfon for 48 h, the AChE activity was assayed by spectrometry and apoptosis was determined by flow cytometry in which the cells were harvested, stained with annexin V-FITC and PI and then analyzed. (A–D) Representative results from one of three independent experiments of cells treated with trichlorfon at concentrations of 0 μM (control) (A), 50 μM (B), 100 μM (C), and 200 μM (D). The quadrant of each plot showed the viable cells appearing as annexin- and PI-negative (annexin⁻/PI⁻, lower left), early apoptotic cells (annexin⁺/PI⁻, lower right), late apoptotic and necrotic cells (annexin⁺/PI⁺, upper right), and not necrotic cells (annexin⁻/PI⁺, upper left). (E) Data are presented as the sum of % apoptotic cells in both early apoptosis (annexin⁺/PI⁻) and late apoptosis (annexin⁺/PI⁺). Values shown are mean ± S.D. (bars) from three independent experiments, *$p < 0.05$. (F) Data are presented as a percentage of AChE activity in control cells treated with 0.1% DMSO (v/v). The basal AChE activity in control cells was defined as 21.40 ± 0.96 nmol acetylthiocholine hydrolyzed/min/mg protein. Data are mean ± S.D. (bars) from three independent tests. *$p < 0.05$, **$p < 0.01$.
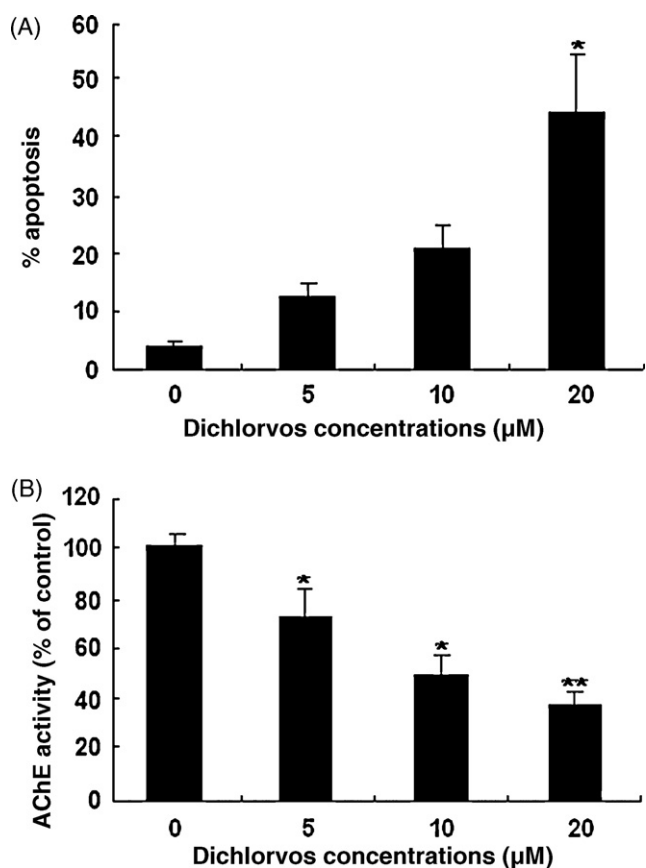
Fig. 2. Induction of apoptosis and inhibition of AChE by dichlorvos in a dose-dependent manner. After cells were treated with a range of concentrations of dichlorvos (0–20 μM) for 48 h, apoptosis was determined by flow cytometry and AChE activity was assayed by spectrometry. (A) Values of % apoptosis shown are mean ± S.D. (bars) from three independent experiments, *$p < 0.05$. (B) Data are presented as a percentage of AChE activity in control cells treated with 0.1% DMSO (v/v). The basal AChE activity in control cells was defined as 21.40 ± 0.96 nmol acetylthiocholine hydrolyzed/min/mg protein. Data are mean ± S.D. (bars) from three independent tests. *$p < 0.05$, **$p < 0.01$.

Fig. 4. Expression of caspase-3, p53, caspase-12, and Bcl-2 in SH-SY5Y cells. The cells were treated with 200 μM trichlorfon for 48 h. Cell lysates were prepared and separated on SDS-PAGE and transferred onto a nitrocellulose membrane. The expression of caspase-3 (32 kDa), caspase-12 (55 kDa), Bcl-2 (27 kDa) and p53 (53 kDa) was visualized by Western blot analysis. Experiments were repeated three times with consistent results. Western blot analysis showed bands of 32 kDa (procaspase-3), 17 kDa (activated caspase-3), 55 kDa (procaspase-12), and 42 kDa (activated caspase-12). An increase in 17 kDa and 42 kDa band intensity was seen following treatment with trichlorfon. Compared to control cells, treated cells had markedly lower Bcl-2 protein expression, and markedly increased p53 protein expression. There was no significant difference in β-actin levels between treated cells and the control.

apoptotic cells (~70%) (Fig. 1E). However, dichlorvos also induced apoptosis in a dose-dependent manner and the higher concentration (20 μM) caused a significant increase in the percentage of apoptotic cells (~45%) (Fig. 2A). As both trichlorfon and its hydrolytic degradation product dichlorvos are organophosphorus pesticides that have cholinergic toxicity, we determined AChE activity in cells treated with these pesticides meanwhile. The results showed that trichlorfon at concentrations of 50, 100, and 200 μM inhibited AChE activity in cells by ~36%, ~48%, and ~51%, respectively (Fig. 1F), while dichlorvos at 5, 10, and 20 μM inhibited the activity respectively by ~27%, ~49%, and ~63% (Fig. 2B), both of which showed a positive relationship between the rate of apoptosis and the rate of AChE inhibition induced by the two pesticides.
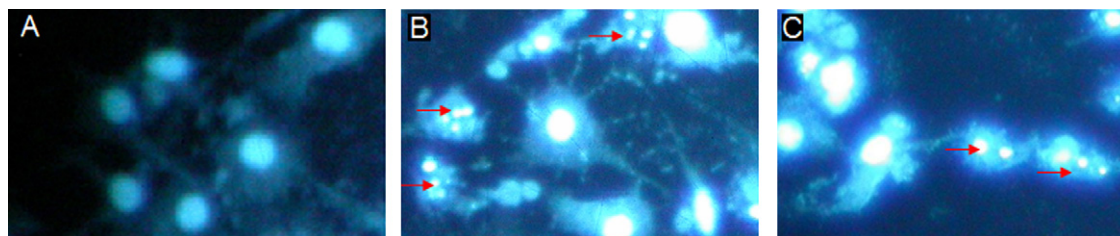
This suggests that the cholinergic toxicity of these OP pesticides is related to the trichlorfon/dichlorvos-induced apoptosis.

Changes in nuclear morphology were assessed using Hoechst 33342. Control cells were intact and their nuclei had dispersed fluorescence (Fig. 3). In contrast, cells treated with both 200 μM of trichlorfon and 20 μM of dichlorvos had condensed chromatin, some of which was assembled at the nuclear membrane, and produced more chromophil granules (Fig. 3). This suggests that these features of treated cells are characteristic of trichlorfon/dichlorvos-induced apoptosis. As seen from the results, both trichlorfon and dichlorvos can induce cell apoptosis and inhibit AChE activity in a concentration-dependent manner. However, it appeared that trichlorfon is less toxic to the cells and trichlorfon at 200 μM induced more cell apoptosis, we therefore used this concentration of trichlorfon in subsequent experiments to determine the mechanism of trichlorfon-induced apoptosis.

Fig. 3. Nuclear fluorescence in SH-SY5Y cells. Cells were treated with 0.1% DMSO (v/v) (control) (A), 200 μM trichlorfon (B), and 20 μM dichlorvos (C) for 48 h, incubated in the dark in 10 μg/ml Hoechst 33342 solution for 20 min, then fixed for 10 min in 90% methanol. Arrowheads indicate late stage apoptotic nuclei. Photos are at 600× magnification.
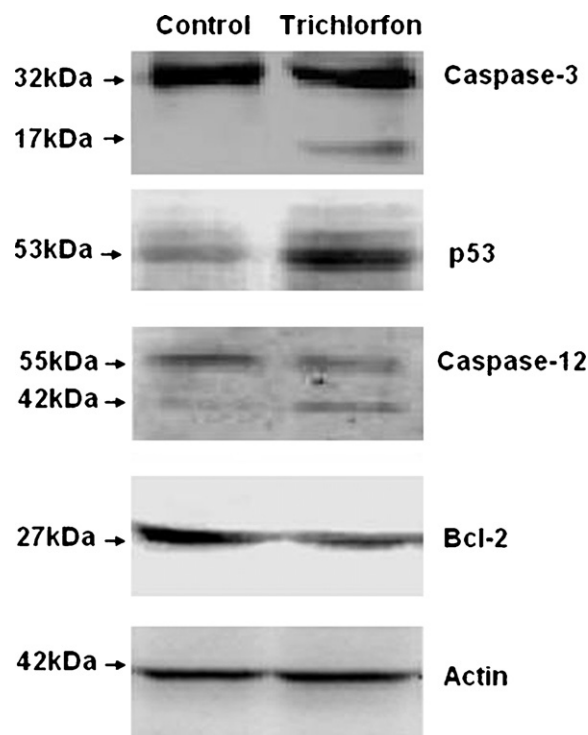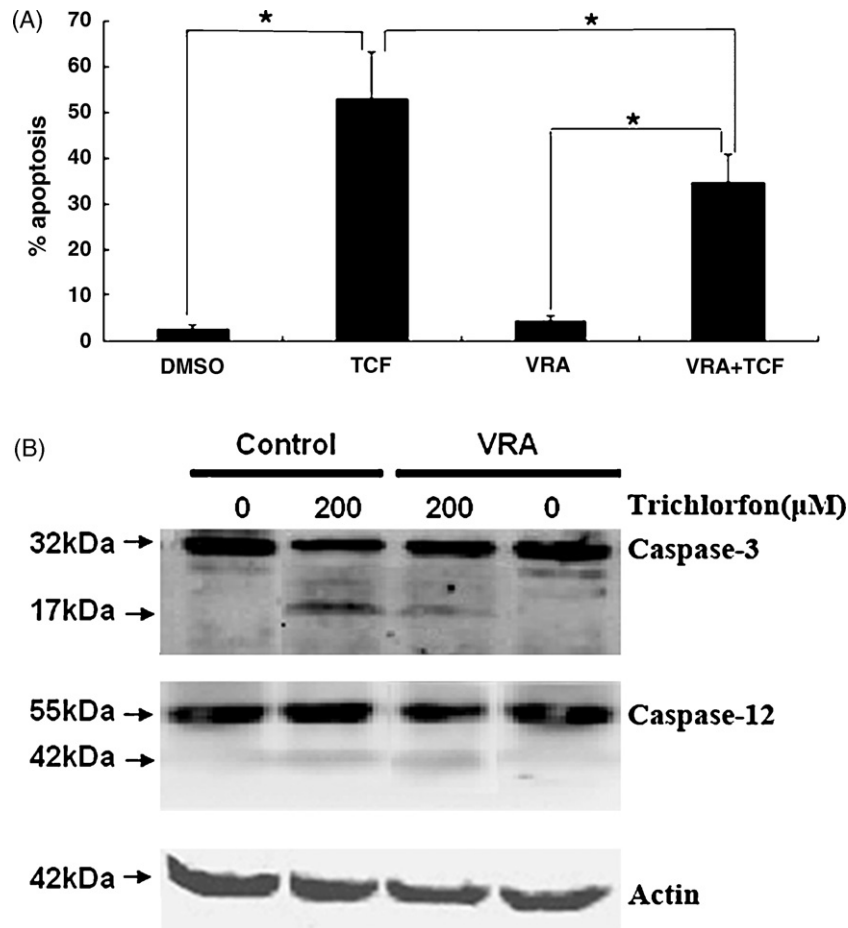
Fig. 5. VRA (verapamil + 2-APB + ruthenium red) reduced percent apoptosis and up-regulation of caspase-3 and caspase-12 protein expression in trichlorfon-treated SH-SY5Y cells. Cells were incubated with 200 μM trichlorfon (TCF) for 48 h in the presence, or absence, of 10 μM VRA for 2 h. (A) Cell apoptosis measured using annexin V/PI staining. Results are means ± S.D., *$p < 0.05$. (B) Cell lysates prepared and separated on SDS-PAGE and transferred onto a nitrocellulose membrane. VRA markedly increased expression of caspase-3 (32 kDa) and caspase-12 (55 kDa) but decreased expression of activated caspase-3 (17 kDa) and caspase-12 (42 kDa). VRA had no effect on β-actin levels.

3.3. Expression of proteins relative to trichlorfon-induced apoptosis

To explore the mechanism through which trichlorfon-induced apoptosis in SH-SY5Y cells, we used Western blot analysis to examine changes in the amount of apoptosis-related proteins, including caspase-3, caspase-12, p53 and Bcl-2. Caspase-3 and caspase-12 showed bands of 32 kDa (procaspase-3), 17 kDa (activated caspase-3), 55 kDa (procaspase-12) and 42 kDa (activated caspase-12) (Fig. 4). An increase in 17 and 42 kDa band intensity was seen following treatment with 200 μM of trichlorfon. Compared to control cells, Bcl-2 protein expression markedly decreased, whereas p53 protein expression markedly increased in trichlorfon-treated cells. This suggests that trichlorfon may induce apoptosis partly via an ER pathway.

3.4. Trichlorfon induced changes in calcium concentration

$[Ca^{2+}]_i$ increased significantly in trichlorfon-treated cells compared to the control ($p < 0.01$) (Table 2). To determine whether Ca^{2+} is involved in apoptosis, we pre-treated cells with "VRA"; a combination of 10 μM verapamil (an L-type Ca^{2+} channel blocker), 10 μM ruthenium red (a potent ryanodine receptor [RyR] inhibitor), and 10 μM 2-APB (an inositol trisphosphate [IP$_3$] receptor [IP$_3$R] inhibitor), before treating them with 200 μM trichlorfon for 48 h. Pre-treatment with 10 μM VRA for 2 h significantly ($p < 0.05$) decreased percent apoptosis (Fig. 5), increased expression of

caspase-3 (32 kDa) and caspase-12 (55 kDa), and decreased activated caspase-3 (17 kDa) and caspase-12 (42 kDa), compared to cells treated with trichlorfon alone (Fig. 5). There was no significant difference in percent apoptosis, protein expression or $[Ca^{2+}]_i$ levels between VRA-treated cells and control cells after 2 h (Table 2).

3.5. Effect of PMA on trichlorfon-induced apoptosis

SH-SY5Y cells were pre-treated with 100 ng/ml phorbol 12-myristate 13-acetate (PMA) for 16 h followed by 200 μM trichlorfon for 48 h, after which cell apoptosis and the expression of different proteins were detected as described above. Pre-treatment with PMA significantly decreased percent apoptosis compared to cells treated with trichlorfon alone ($p < 0.05$) and percent apoptosis of PMA-treated cells was not significantly different to that of control cells (Fig. 6A). In addition, Western blot analysis indi-

Table 2
Effects of trichlorfon on calcium concentration in SH-SY5Y cells.

Treatment	$[Ca^{2+}]_i$ (nM)
Control (DMSO)	131.16 ± 12.23
Trichlorfon	301.47 ± 22.56**
VRA + trichlorfon	183.42 ± 19.73
VRA	160.86 ± 18.75

VRA: verapamil + ruthenium red + 2-APB.
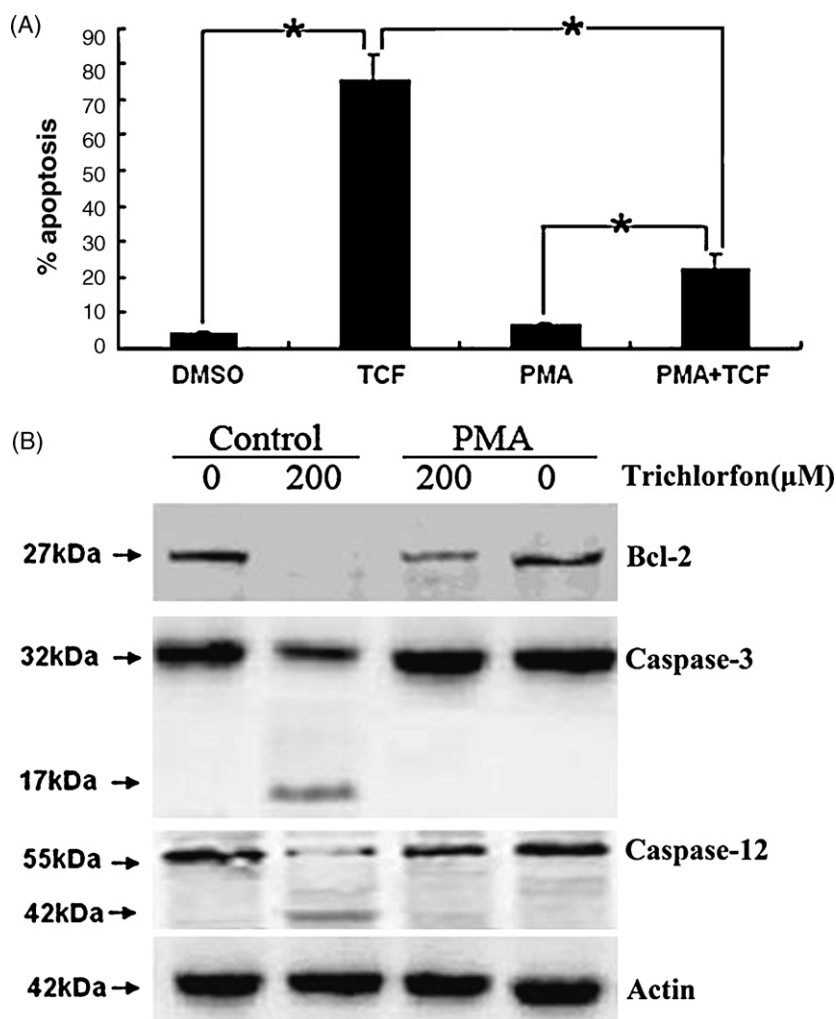** p-Value of treated cells was <0.01 vs. control, $n = 3$.

Fig. 6. PMA reduced percent apoptosis and up-regulation of Bcl-2, caspase-3, and caspase-12 protein expression in SH-SY5Y cells. Cells were incubated with 200 μM trichlorfon (TCF) for 48 h in the presence or absence of 100 ng/ml PMA for 16 h. (A) Cell apoptosis measured using annexin V/PI staining. Results are mean ± S.D., *$p < 0.05$. (B) Cell lysates prepared and separated on SDS-PAGE and transferred onto a nitrocellulose membrane. The expression of Bcl-2 (27 kDa), caspase-3 (32 kDa), and caspase-12 (55 kDa) was visualized by Western blot analysis. PMA markedly increased the protein levels of Bcl-2 (27 kDa), caspase-3 (32 kDa), and caspase-12 (55 kDa), decreased activated caspase-3 (17 kDa) and activated caspase-12 (42 kDa) but had no effect on β-actin levels.

cated that pre-treatment with PMA markedly increased the protein levels of Bcl-2, caspase-3 (32 kDa) and caspase-12 (55 kDa), but decreased activated caspase-3 (17 kDa) and activated caspase-12 (42 kDa), compared to cells treated with trichlorfon alone. Pre-treatment with PMA had no significant effect on β-actin levels (Fig. 6B).

4. Discussion

Our results demonstrate that trichlorfon inhibited SH-SY5Y cell viability in a concentration dependent manner. Analysis of annexin V/PI fluorescence indicated that cells treated with trichlorfon showed distinct changes compared to control cells. Compared with trichlorfon, its hydrolytic degradation product dichlorvos-induced apoptosis at lower concentrations and inhibited AChE activity; however, more apoptotic cells were induced by trichlorfon at higher concentrations. To further elucidate the apoptosis mechanism, we focused on the molecular events involved in apoptosis in SH-SY5Y induced by trichlorfon.

The ER is a vitally important intracellular organelle comprised of an extensive network of cisternae and microtubules that stretches from the nuclear envelope to the cell surface in all eukaryotic cells

[20,21]. Various stresses, including expression of mutant proteins, viral infection, energy or nutrient deprivation, extreme environmental conditions, alterations in redox or glycosylation status and calcium release from the lumen of the ER, disrupt proper function of the ER and cause so-called ER stress.

The first ER-associated caspase, caspase-12, was discovered by Nakagawa and Yuan [22]. These authors demonstrated that caspase-12 activation is induced by ER stress, such as that caused by treatment with thapsigargin and tunicamycin, and results in cell death. Current models suggest that caspase-12 acts as the initiator caspase in ER stress. Caspase-12 can be cleaved by IRE1α/TRAF2, calpain, or caspase-7, or induced by ATF6. Cleaved caspase-12 can either directly process caspase-9 or cleave Bap31, resulting in mitochondrial permeabilization, cytochrome *c* release, and Apaf-1-mediated caspase-9 processing, ultimately leading to caspase-3 cleavage [23–25]. However, although the role of caspase-12 in ER stress-induced apoptosis of murine cells is well established, there is also evidence that the human caspase-12 gene is nonfunctional [26]. Some authors suggest that ER stress in humans may activate the mitochondrial apoptosis pathway [27–29]. Our results indicate that caspase-12 and caspase-3 are activated in trichlorfon-induced apoptosis in SH-SY5Y cells, suggesting that trichlorfon can induce apoptosis via an ER-dependent pathway.

The ER is a dynamic Ca^{2+} reservoir and consequently plays an important role in physiological signaling activated by both electrical and chemical cell stimulation [30,31]. Moreover, the ER plays a key role in redistributing Ca^{2+} ions within the cell; the excitable ER membrane forms propagating cytosolic Ca^{2+} waves and the ER lumen functions as an intracellular Ca^{2+} channel [32]. Dynamic changes in free Ca^{2+} concentration within the ER lumen determines the ER function as a Ca^{2+} signaling organelle and regulates the activity of intra-ER resident enzymatic cascades. Our results show that $[Ca^{2+}]_i$ increased in SH-SY5Y cells after treatment with trichlorfon.

When the release of Ca^{2+} from the ER and outer membrane was blocked, $[Ca^{2+}]_i$ was maintained at low levels, while at the same time, percentage apoptosis and activated caspase-12 decreased compared to trichlorfon-treated cells. Therefore, we speculate that Ca^{2+} may trigger apoptosis and the activation of caspase-12 in cells treated with trichlorfon.

The anti-apoptotic Bcl-2 family member Bcl-2 can block apoptosis in mitochondria, and is reported to inhibit apoptosis in a variety of cell types [33]. Bcl-2 is located in the membranes of mitochondria, the ER, and the nucleus of different cell types [34]. Ghribi et al. demonstrated that levels of Bcl-2 decreased in mitochondrial and ER fractions derived from brain tissue decreased following the administration of aluminum maltolate to young adult rabbits [35]. Treatment of primary cultures of human neurons with Aβ (1–40) initiates a down-regulation of Bcl-2 expression [36]. Previous study demonstrated that down regulation of Bcl-2 was an early event in the process of ER stress-mediated apoptosis in cortical neurons and then highlighted the potential importance of the mitochondria as pivotal mediator of apoptosis in response to neuronal ER stress [37]. These findings also suggested that an apoptotic crosstalk between ER and mitochondria was controlled by Bcl-2 [38]. Our results show that treatment with trichlorfon induces a marked decrease in Bcl-2 levels in SH-SY5Y cells, which suggests that there may exist a crosstalk between ER and mitochondria in trichlorfon-induced apoptosis.

PMA is the activator of protein kinase C (PKC). PMA significantly suppressed trichlorfon-induced apoptosis, and also decreased expression of activated caspase-3 and caspase-12 compared to cells treated with trichlorfon alone. Expression of Bcl-2 increased after pre-treatment with PMA. Though Bcl-2 is regarded as an important factor in mitochondria, it is found on other inner membranes, such as the ER and the nuclear membrane [39]. Studies show that Bcl-2 can reduce the release of calcium from the ER, thus dampening fluctuation in $[Ca^{2+}]_i$ [40]. Recent research has found that Bcl-2 can directly act on IP3R, suppressing both the opening of the ion channel and calcium release from the ER [41]. Therefore, we speculate that PMA may activate Bcl-2, stabilize calcium homeostasis and decrease cell stress, thereby decreasing trichlorfon-induced apoptosis.

In conclusion, our results demonstrate that trichlorfon induced a concentration dependent apoptosis of SH-SY5Y cells. We speculate that treatment with trichlorfon caused $[Ca^{2+}]_i$ to increase, activated caspase-12 followed by caspase-3, and finally triggered apoptosis partly through the ER pathway.

Conflict of interest

The authors declare that there are no conflicts of interest.

Acknowledgments

References

[1] K. Grave, M. Engelstad, N.E. Soli, Utilization of dichlorvos and trichlorfon in salmonid farming in Norway during 1981–1988, Acta Vet. Scand. 32 (1991) 1–7.

[2] R.E. Becker, J.A. Colliver, S.J. Markwell, P.L. Moriearty, L.K. Unni, S. Vicari, Double-blind, placebo-controlled study of metrifonate, an acetylcholinesterase inhibitor, for Alzheimer disease, Alzheimer Dis. Assoc. Disord. 10 (1996) 124–131.

[3] W.J. Krall, J.J. Sramek, N.R. Cutler, Cholinesterase inhibitors: a therapeutic strategy for Alzheimer disease, Ann. Pharmacother. 33 (1999) 441–450.

[4] V.C. Hinz, S. Grewig, B.H. Schmidt, Metrifonate induces cholinesterase inhibition exclusively via slow release of dichlorvos, Neurochem. Res. 21 (1996) 331–337.

[5] E.J. Olajos, I. Rosenblum, F. Coulston, N. Strominger, The dose response relationship of trichlorfon neurotoxicity in hens, Ecotoxicol. Environ. Saf. 3 (1979) 245–255.

[6] A.E. Czeizel, C. Elek, S. Gundy, J. Metneki, E. Nemes, A. Reis, K. Sperling, L. Timar, G. Tusnady, Z. Viragh, Environmental trichlorfon and cluster of congenital abnormalities, Lancet 341 (1993) 539–542.

[7] A.T. Doherty, S. Ellard, E.M. Parry, J.M. Parry, A study of the aneugenic activity of trichlorfon detected by centromere-specific probes in human lymphoblastoid cell lines, Mutat. Res. 372 (1996) 221–231.

[8] S. Cukurcam, F. Sun, I. Betzendahl, I.D. Adler, U. Eichenlaub-Ritter, Trichlorfon predisposes to aneuploidy and interferes with spindle formation in in vitro maturing mouse oocytes, Mutat. Res. 564 (2004) 165–178.

[9] J.F. Zhou, W. Zhou, S.M. Zhang, Y.E. Luo, H.H. Chen, Oxidative stress and free radical damage in patients with acute dipterex poisoning, Biomed. Environ. Sci. 17 (2004) 223–233.

[10] B. Karademir Catalgol, S. Ozden, B. Alpertunga, Effects of trichlorfon on malondialdehyde and antioxidant system in human erythrocytes, Toxicol. In Vitro 21 (2007) 1538–1544.

[11] A. Mehl, T.M. Schanke, A. Torvik, F. Fonnum, The effect of trichlorfon and methylazoxymethanol on the development of guinea pig cerebellum, Toxicol. Appl. Pharmacol. 219 (2007) 128–135.

[12] M. Ehrich, B. Veronesi, Esterase comparison in neuroblastoma cells of human and rodent origin, Clin. Exp. Pharmacol. Physiol. 22 (1995) 385–386.

[13] R.C. Duke, D.M. Ojcius, J.D. Young, Cell suicide in health and disease, Sci. Am. 275 (1996) 80–87.

[14] J.P. Cobb, R.S. Hotchkiss, I.E. Karl, T.G. Buchman, Mechanisms of cell injury and death, Br. J. Anaesth. 77 (1996) 3–10.

[15] V. Gorun, I. Proinov, V. Baltesuc, G. Balaban, O. Barzu, Modified Ellman procedure for assay of cholinesterase in crude enzymatic preparations, Anal. Biochem. 86 (1978) 324–326.

[16] X.H. Li, Y.J. Wu, Characteristics of lysophosphatidylcholine-induced Ca^{2+} response in human neuroblastoma SH-SY5Y cells, Life Sci. 80 (2007) 886–892.

[17] P.A. Chang, Y.J. Wu, W. Li, X.F. Leng, Effect of carbamate esters on neurite outgrowth in differentiating human SK-N-SH neuroblastoma cells, Chem. Biol. Interact. 159 (2006) 65–72.

[18] M.M. Bradford, A rapid and sensitive method for the quantitation of microgram quantities of protein utilizing the principle of protein-dye binding, Anal. Biochem. 72 (1976) 248–254.

[19] L. Masoud, C. Vijayasarathy, M. Fernandez-Cabezudo, G. Petroianu, A.M. Saleh, Effect of malathion on apoptosis of murine L929 fibroblasts: a possible mechanism for toxicity in low dose exposure, Toxicology 185 (2003) 89–102.

[20] O. Baumann, B. Walz, Endoplasmic reticulum of animal cells and its organization into structural and functional domains, Int. Rev. Cytol. 205 (2001) 149–214.

[21] O.V. Gerasimenko, J.V. Gerasimenko, R.R. Rizzuto, M. Treiman, A.V. Tepikin, O.H. Petersen, The distribution of the endoplasmic reticulum in living pancreatic acinar cells, Cell Calcium 32 (2002) 261–268.

[22] T. Nakagawa, J. Yuan, Cross-talk between two cysteine protease families. Activation of caspase-12 by calpain in apoptosis, J. Cell. Biol. 150 (2000) 887–894.

[23] W.C. Earnshaw, L.M. Martins, S.H. Kaufmann, Mammalian caspases: structure, activation, substrates, and functions during apoptosis, Annu. Rev. Biochem. 68 (1999) 383–424.

[24] T. Yoneda, K. Imaizumi, K. Oono, D. Yui, F. Gomi, T. Katayama, M. Tohyama, Activation of caspase-12, an endoplastic reticulum (ER) resident caspase, through tumor necrosis factor receptor-associated factor 2-dependent mechanism in response to the ER stress, J. Biol. Chem. 276 (2001) 13935–13940.

[25] R.V. Rao, H.M. Ellerby, D.E. Bredesen, Coupling endoplasmic reticulum stress to the cell death program, Cell Death Differ. 11 (2004) 372–380.

[26] H. Fischer, U. Koenig, L. Eckhart, E. Tschachler, Human caspase 12 has acquired deleterious mutations, Biochem. Biophys. Res. Commun. 293 (2002) 722–726.

[27] J. Hacki, L. Egger, L. Monney, S. Conus, T. Rosse, I. Fellay, C. Borner, Apoptotic crosstalk between the endoplasmic reticulum and mitochondria controlled by Bcl-2, Oncogene 19 (2000) 2286–2295.

[28] M.G. Annis, N. Zamzami, W. Zhu, L.Z. Penn, G. Kroemer, B. Leber, D.W. Andrews, Endoplasmic reticulum localized Bcl-2 prevents apoptosis when redistribution of cytochrome c is a late event, Oncogene 20 (2001) 1939–1952.

[29] M.C. Wei, W.X. Zong, E.H. Cheng, T. Lindsten, V. Panoutsakopoulou, A.J. Ross, K.A. Roth, G.R. MacGregor, C.B. Thompson, S.J. Korsmeyer, Proapoptotic BAX and BAK: a requisite gateway to mitochondrial dysfunction and death, Science 292 (2001) 727–730.

[30] M.D. Bootman, O.H. Petersen, A. Verkhratsky, The endoplasmic reticulum is a focal point for co-ordination of cellular activity, Cell Calcium 32 (2002) 231–234.

[31] A. Verkhratsky, O.H. Petersen, The endoplasmic reticulum as an integrating signalling organelle: from neuronal signalling to neuronal death, Eur. J. Pharmacol. 447 (2002) 141–154.

[32] H. Mogami, K. Nakano, A.V. Tepikin, O.H. Petersen, Ca^{2+} flow via tunnels in polarized cells: recharging of apical Ca^{2+} stores by focal Ca^{2+} entry through basal membrane patch, Cell 88 (1997) 49–55.

[33] Y. Terui, Y. Furukawa, J. Kikuchi, S. Iwase, K. Hatake, Y. Miura, Bcl-x is a regulatory factor of apoptosis and differentiation in megakaryocytic lineage cells, Exp. Hematol. 26 (1998) 236–244.

[34] B. Fadeel, B. Zhivotovsky, S. Orrenius, All along the watchtower: on the regulation of apoptosis regulators, FASEB J. 13 (1999) 1647–1657.

[35] O. Ghribi, D.A. DeWitt, M.S. Forbes, M.M. Herman, J. Savory, Co-involvement of mitochondria and endoplasmic reticulum in regulation of apoptosis: changes in cytochrome c, Bcl-2 and Bax in the hippocampus of aluminum-treated rabbits, Brain Res. 903 (2001) 66–73.

[36] E. Paradis, H. Douillard, M. Koutroumanis, C. Goodyer, A. LeBlanc, Amyloid beta peptide of Alzheimer's disease downregulates Bcl-2 and upregulates bax expression in human neurons, J. Neurosci. 16 (1996) 7533–7539.

[37] W. Elyaman, F. Terro, K. Suen, C. Yardin, R. Chang, J. Hugon, BAD and Bcl-2 regulation are early events linking neuronal endoplasmic reticulum stress to mitochondria-mediated apoptosis, Mol. Brain Res. 109 (2002) 233–238.

[38] J. Häcki, L. Egger, L. Monney, S. Conus, T. Rosśe, I. Fellay, C. Borner, Apoptotic crosstalk between the endoplasmic reticulum and mitochondria controlled by Bcl-2, Oncogene 19 (2000) 2286–2295.

[39] W.C. Lam, A.H. Maki, J.R. Casas-Finet, J.W. Erickson, B.P. Kane, R.C. Sowder 2nd, L.E. Henderson, Phosphorescence and optically detected magnetic resonance investigation of the binding of the nucleocapsid protein of the human immunodeficiency virus type 1 and related peptides to RNA, Biochemistry 33 (1994) 10693–10700.

[40] C.W. Distelhorst, T.S. McCormick, Bcl-2 acts subsequent to and independent of Ca^{2+} fluxes to inhibit apoptosis in thapsigargin- and glucocorticoid-treated mouse lymphoma cells, Cell Calcium 19 (1996) 473–483.

[41] C. Li, X. Wang, H. Vais, C.B. Thompson, J.K. Foskett, C. White, Apoptosis regulation by Bcl-x(L) modulation of mammalian inositol 1,4,5-trisphosphate receptor channel isoform gating, Proc. Natl. Acad. Sci. U.S.A. 104 (2007) 12565–12570.